Supplementary Information

The role of sacral slope in the progression of a bilateral spondylolytic defect at L5 to spondylolisthesis: A biomechanical investigation using finite element analysis

Calibration of material property values used in the finite element (FE) models

Although Heuer *et al.* (2007) presented *in vitro* biomechanical testing data for L4-L5 segments; the geometry of L3-L4 FSU was used in the present study for calibration purposes. [1] In the present study, an indirect calibration approach was adopted, where the CT data used in building the FE model were obtained from a 26 year old healthy male subject, and in vitro biomechanical testing data were obtained from Heuer *et al.* (2007) study.[1] In the intact state, L4-L5 lumbar lordosis in the FE geometry was different from that reported in the in vitro study. An attempt was made in the FE software to reposition the L4 vertebra relative to the L5 vertebra in order to obtain a lumbar lordosis match, but this resulted in distraction and misalignment of articulating bony pillars of the facet joints. Lumbar lordosis has a bearing on angular range of motion (RoM) and neutral zone (NZ) measurements. Therefore, an L3-L4 FSU was modelled instead, for which lumbar lordosis was manipulated (with relative ease) to match with the experimental data without disorienting the facet joints.

To simulate loads and boundary constraints described by Heuer *et al.* (2007), a centre node on the L4 inferior endplate was constrained from all movements in rotational and translational degrees of freedom. [1] Unconstrained pure moments were applied to the L3 superior endplate using a cross-beam construct attached to it (Figure S1).
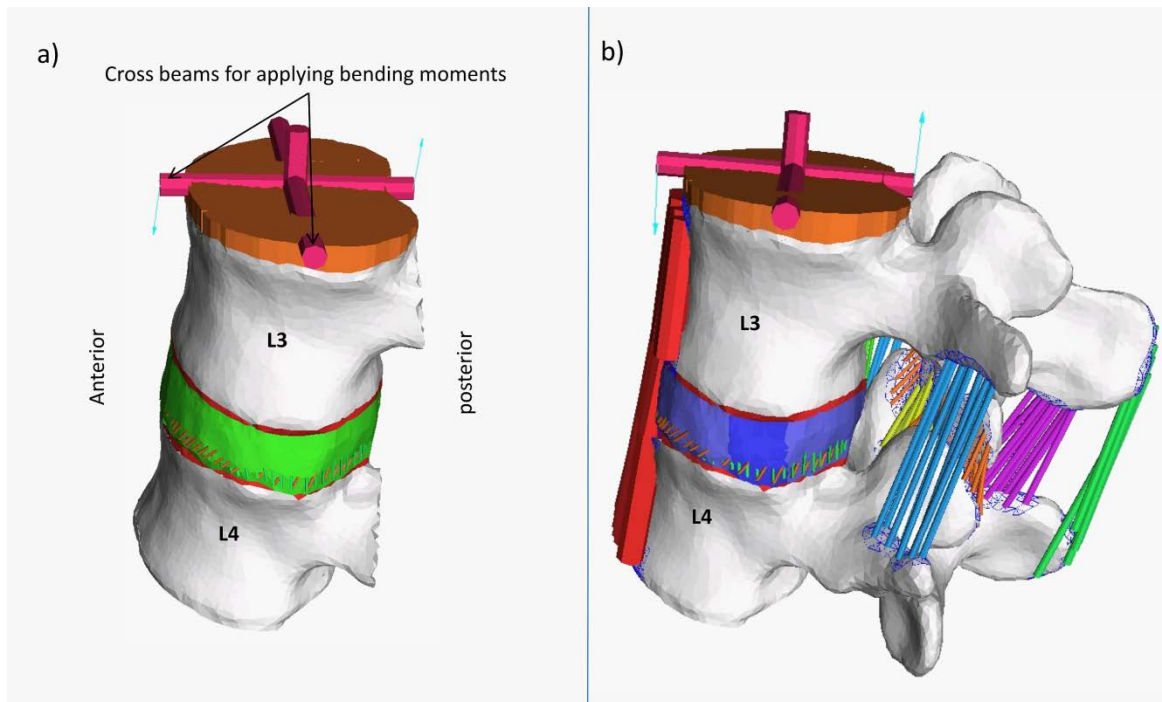
Figure S1. A multi-stage calibration approach was used to calibrate material property values assigned to various anatomical structures in the finite element (FE) models. a) First stage of the calibration study: A nucleotomised FE model of L3-L4 segment was used for calibrating material property values assigned to the annulus fibrosus. b) Last stage of the calibration study: An intact FE model of L3-L4 functional spinal unit was used to calibrate material property values assigned to the last anatomical structure added to the model (supraspinous ligaments). See Figure S3 for the sequential addition of anatomical structures.

Loads were incrementally increased (1Nm, 2.5Nm, 5Nm, 7.5Nm, and 10Nm) and nonlinear static solves were run in Strand7 (incorporating geometric, boundary, and material non-linearities) to generate results for each stage of the increment. Range of motion (RoM) values at different load increments were evaluated from the solved FE models and compared with the *in vitro* RoM results. The deviations in $RoM_{numerical}$ from $RoM_{in\text{-}vitro}$ at different loads were quantified, and a closed loop optimisation algorithm was formulated to achieve a RoM for the FE-model that was similar to the *in vitro* data (Figure S2). A new parameter called Calibration Factor (λ_{cal}) was defined for this purpose, which captured the average deviation in $RoM_{numerical}$ at different loads for the four bending motions combined.

Supplementary Information

$$d_i = \frac{\text{RoM}_{numerical|i} - \text{RoM}_{in-vitro|i}}{\text{RoM}_{in\,vitro|i}} \qquad (1)$$

where d_i was calculated at the corresponding W_i bending load

W_i = ±1Nm, ±2.5Nm, ±5Nm, ±7.5Nm, ±10.0Nm   (i =1, 2, 3, 4, 5)

Load-weighted average deviation was calculated as:

$$D_{avg|j} = \frac{\sum_{i=1}^{5} W_i . d_i}{\sum_{i=1}^{5} W_i} \qquad (2)$$

where j corresponds to different bending motions

j =1 (Flexion)

j =2 (Extension)

j =3 (Right lateral bending)

j =4 (Left axial torsion)

Calibration Factor (λ_{cal}) was defined as follows:

$$\lambda_{cal} = 1 + \frac{\sum_{j=1}^{4} D_{avg|j}}{4} \qquad (3)$$
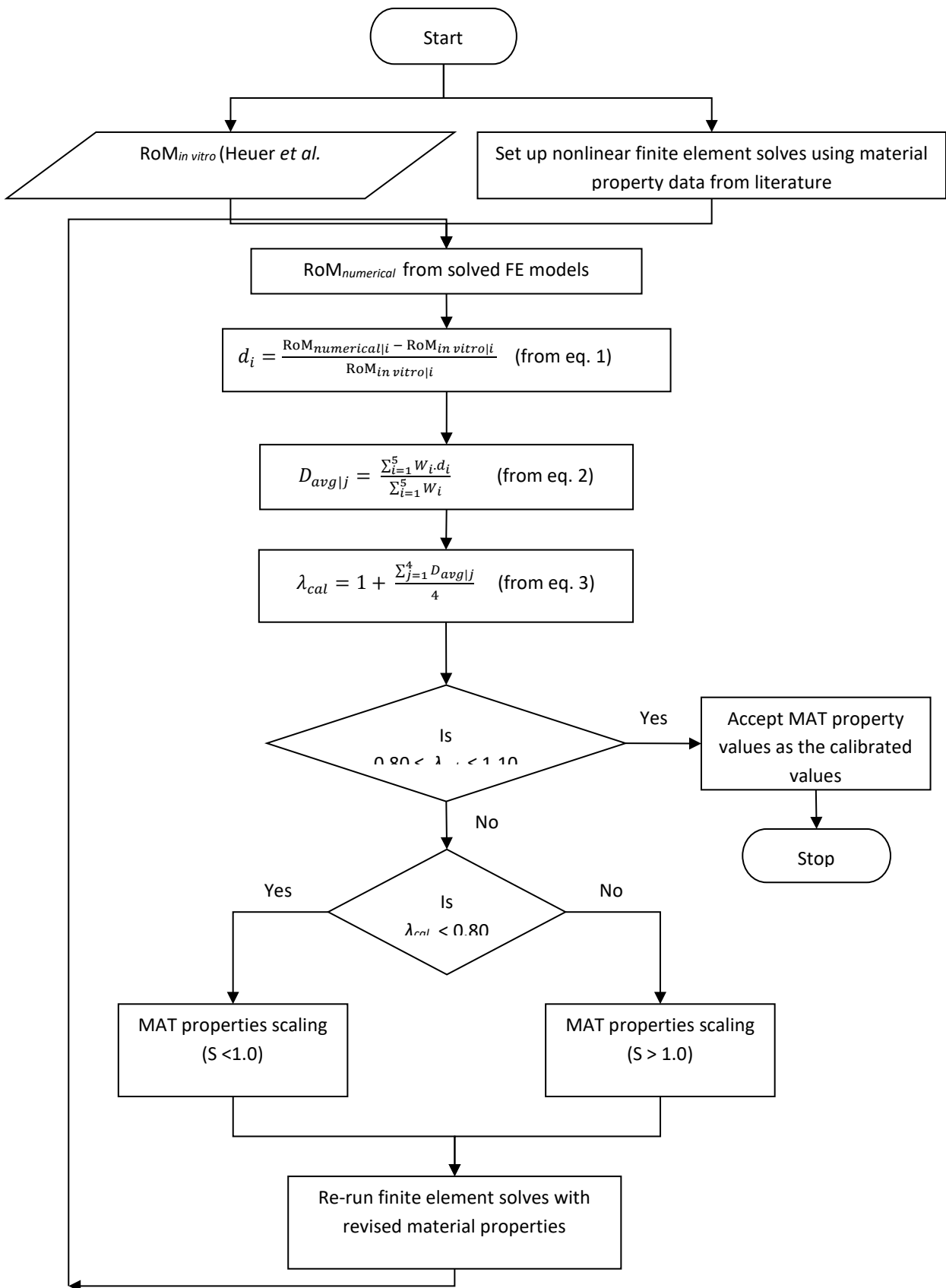
Figure S2. A schema of the optimisation algorithm used for calibrating material property values for various anatomical structures in the finite element model of human lumbar spine.

Supplementary Information

The last stage of the anatomical reduction in the *in vitro* study was treated as the starting point in the calibration study.[1] Anatomical structures were added in a stepwise manner, and the process was repeated for calibrating material property values of the structure added (Figure S3).

Stage 1: Finite element model stripped down to L3-L4 vertebral bodies + annulus (nucleotomised)

↓

Stage 2: Nucleus pulposus added

↓

Stage 3: Anterior longitudinal ligaments added

↓

Stage 4: Posterior longitudinal ligaments added

↓

Stage 5: Vertebral arches added to L3 and L4

↓

Stage 6: Capsular ligaments added

↓

Stage 7: Ligamentum flavum added

↓

Stage 8: Interspinous ligaments added

↓

Stage 9: Supraspinous ligaments added (Intact finite element model of L3-L4 lumbar spine segment)

Figure S3. The sequence of stepwise addition of anatomical structures adopted in the present calibration study.

Supplementary Information

Material property values for the cortical and cancellous bone, the three regions of endplates, transverse, iliolumbar, and lumbosacral ligaments could not be calibrated using this approach; and therefore, uncalibrated values extracted directly from the literature were used in the models (Table S1).

Table S1. Material property values assigned to the uncalibrated elements in the finite element models. Due to lack of published data on Iliolumbar and Lumbosacral ligaments, these were assigned the same material properties as the Anterior Longitudinal Ligament.

	Element type	**Material model**	**Material property values (uncalibrated)** E : Elastic Modulus (MPa) G: Shear Modulus (MPa) v: Poisson's Ratio d: Diameter (millimetres) k: Stiffness (N/mm) ε: Strain %	**Source literature**
Cancellous bone	4-noded tetrahedral	Orthotropic	$E\_xx = 140$; $E\_yy = 140$; $E\_zz = 200$; $G\_xy = 48.3$; $G\_yz = 48.3$; $G\_xz = 48.3$; $v\_xx = 0.45$; $v\_yy = 0.315$; $v\_zz = 0.315$	[2]
Cortical bone	4-noded tetrahedral	Orthotropic	$E\_xx = 11300$; $E\_yy = 11300$; $E\_zz = 22000$; $G\_xy = 3800$; $G\_yz = 5400$; $G\_xz = 5400$; $v\_xx = 0.484$; $v\_yy = 0.203$; $v\_zz = 0.203$	[2]
Endplates inner	4-noded tetrahedral	Isotropic	E = 2000	[3]
Endplates middle	4-noded tetrahedral	Isotropic	E = 6000	[3]
Endplates outer	4-noded tetrahedral	Isotropic	E = 12000	[3]
Intertransverse ligaments	Beam	Non-linear elastic	N = 16 per level d = 1.0 $E_t = 10.0 (\varepsilon < 18\%), 58.7 (\varepsilon > 18\%)$; v = 0.3	[4]

Supplementary Information

Iliolumbar ligaments	Beam	Non-linear elastic	N = 20 d = 1.0 E_t = 7.8(ε< 12%), 20.0(ε>12%); v = 0.3	No literature available
Lumbosacral ligaments	Beam	Non-linear elastic	N = 22 d = 2.0 E_t = 7.8(ε< 12%), 20.0(ε>12%); v = 0.3	No literature available
Nonlinear contact Zero-Gap elements (Pars defect separation)	Beam	Non-linear Zero Gap	k = 5000	[5]

The calibrated material property values for various elements are presented in Table S2.

Table S2. Calibrated material property values for various elements used in the finite element models. To incorporate regional variation in the stiffness properties of annulus fibrosus, the annulus ground substance was divided into five regions with specific local weight factors for each region.[6]

	Element type	Material model	Material property values (calibrated) E: Elastic Modulus (MPa) K: Bulk Modulus (MPa) v: Poisson's Ratio d: Diameter (millimetres) k: Stiffness (N/mm) ε: Strain % C_1, C_2: Mooney-Rivlin constants T: Tension (N)	Source literature for uncalibrated (starting point) material properties
Nucleus pulposus	4-noded tetrahedral	Mooney-Rivlin, 2 parameters	C_1 = 0.006; C_2 = 0.0045; K = 105	[6]

Annulus ground substance
  I.   **Anterior**
  II. **Posterior**
  III. **Lateral**
  IV. **Anterolateral**
  V. **Posterolateral**
	4-noded tetrahedral	Mooney-Rivlin, 2 parameters	I. C_1 = 0.0672, C_2 = 0.0168, K = 1.68
			II. C_1 = 0.0476, C_2 = 0.0119, K = 1.19
			III. C_1 = 0.0364, C_2 = 0.0091, K = 0.91
			IV. C_1 = 0.0476, C_2 = 0.0119, K = 1.19
			V. C_1 = 0.0459, C_2 = 0.0115, K = 1.15
				[6]

Annulus Fibres
  I.   **Layer 1**
  II. **Layer 2**
  III. **Layer 3**
  IV. **Layer 4**
	Beam	Non-linear elastic	I. E_t = 275, v = 0.3
			II. E_t = 242.5, v = 0.3
			III. E_t = 210, v = 0.3
			IV. E_t = 180, v = 0.3
				[7]

Ligaments
  I.   **ALL**
  II. **PLL**
  III. **LF**
  IV. **CL**
  V. **ISL**
  VI. **SSL**
	Beam	Non-linear elastic	I. N = 14 continuous, d = 4.8,
			    E_t = 23.4(ε< 12%), 60(ε>12%), v = 0.3
			II. N = 6 continuous, d = 0.7,
			    E_t = 5(ε< 11%), 10(ε>11%), v = 0.3
			III. N = 18 per level, d = 1.1,
			    E_t = 15(ε<6.2%), 10(ε>6.2%), v = 0.3
			IV. N = 48 per level, d = 0.8,
			    E_t = 7.5(ε< 25%), 32.9(ε>25%), v = 0.3
			V. N = 9 per level, d = 1.2,
			    E_t = 10(ε< 14%), 11.6(ε>14%), v = 0.3
			VI. N = 4 continuous, d = 1.5,
			    E_t = 8(ε< 20%), 15(ε>20%), v = 0.3
				[4]

Nonlinear Point-Contact elements (Facet articulation)	Beam	Non-linear Tension Contact	k = 25 T = 5	[5]

ALL: Anterior Longitudinal Ligament; PLL: Posterior Longitudinal Ligament; LF: Ligamentum Flavum; CL: Capsular Ligament; ISL: Interspinous Ligament; SSL: Supraspinous Ligament

Supplementary Information

References

1. Heuer F, Schmidt H, Klezl Z et al. Stepwise reduction of functional spinal structures increase range of motion and change lordosis angle. Journal of biomechanics 2007; 40: 271-280 DOI: 10.1016/j.jbiomech.2006.01.007
2. Lu YM, Hutton WC, Gharpuray VM. Do bending, twisting, and diurnal fluid changes in the disc affect the propensity to prolapse? A viscoelastic finite element model. Spine 1996; 21: 2570-2579
3. Edwards WT, Zheng Y, Ferrara LA et al. Structural features and thickness of the vertebral cortex in the thoracolumbar spine. Spine 2001; 26: 218-225
4. Kiapour A, Ambati D, Hoy RW et al. Effect of graded facetectomy on biomechanics of Dynesys dynamic stabilization system. Spine 2012; 37: E581-589 DOI: 10.1097/BRS.0b013e3182463775
5. Theoretical Manual: Theoretical Background to the Strand7 Finite Element Analysis System. Sydney: G+D Computing; 2004
6. Schmidt H, Heuer F, Simon U et al. Application of a new calibration method for a three-dimensional finite element model of a human lumbar annulus fibrosus. Clinical biomechanics (Bristol, Avon) 2006; 21: 337-344 DOI: 10.1016/j.clinbiomech.2005.12.001
7. Denoziere G, Ku DN. Biomechanical comparison between fusion of two vertebrae and implantation of an artificial intervertebral disc. Journal of biomechanics 2006; 39: 766-775 DOI: 10.1016/j.jbiomech.2004.07.039